Mechanistic fracture criteria for the failure of human cortical bone

R. K. NALLA[1], J. H. KINNEY[2] AND R. O. RITCHIE*[1]

[1]Materials Sciences Division, Lawrence Berkeley National Laboratory, and Department of Materials Science and Engineering, University of California, Berkeley, California 94720, USA
[2]Department of Preventive and Restorative Dental Sciences, University of California, San Francisco, California 94143, USA
*e-mail: RORitchie@lbl.gov

Published online: 9 February 2003; doi:10.1038/nmat832

A mechanistic understanding of fracture in human bone is critical to predicting fracture risk associated with age and disease. Despite extensive work, a mechanistic framework for describing how the microstructure affects the failure of bone is lacking. Although micromechanical models incorporating local failure criteria have been developed for metallic and ceramic materials[1,2], few such models exist for biological materials. In fact, there is no proof to support the widely held belief that fracture in bone is locally strain-controlled[3,4], as for example has been shown for ductile fracture in metallic materials[5]. In the present study, we provide such evidence through a novel series of experiments involving a double-notch-bend geometry, designed to shed light on the nature of the critical failure events in bone. We examine how the propagating crack interacts with the bone microstructure to provide some mechanistic understanding of fracture and to define how properties vary with orientation. It was found that fracture in human cortical bone is consistent with strain-controlled failure, and the influence of microstructure can be described in terms of several toughening mechanisms. We provide estimates of the relative importance of these mechanisms, such as uncracked-ligament bridging.

Human bone has a complex hierarchical microstructure[6–9] that can be considered at many dimensional scales[6,7]. At the shortest length-scale, it is composed of type-I collagen fibres (up to 15 μm in length, 50–70 nm in diameter) bound and impregnated with carbonated apatite nanocrystals (tens of nanometres in length and width, 2–3 nm in thickness)[6,7]. These mineralized collagen fibres are further organized at a microstructural length-scale into a lamellar structure, with roughly orthogonal orientations of adjacent lamellae (3–7 μm thick)[8]. Permeating this lamellar structure are the secondary osteons[9] (up to 200–300 μm diameter): large vascular channels (up to 50–90 μm diameter) oriented roughly in the growth direction of the bone and surrounded by circumferential lamellar rings. The difficulty in understanding the mechanisms of fracture in bone lies in determining the relative importance of these microstructural hierarchies on crack initiation, subsequent crack propagation and consequent unstable fracture, and in separating their effects on the critical fracture events.

A vital distinction in the definition of the local (precursor) fracture events that cause macroscopic failure is whether they are locally stress- or strain-controlled. Brittle fracture is invariably stress-controlled, for example in structural steels at low temperatures, where cleavage fracture is instigated by the precursor cracking of carbide particles or inclusions[1,2]. Ductile fracture, conversely, is strain-controlled, as in the same steels at higher temperatures where the fracture process involves ductile tearing between such particles or inclusions (with a significant increase in toughness)[2]. Bone fracture is widely regarded as strain-controlled; indeed, most theoretical descriptions of its mechanical behaviour assume this to be the case[3]. However, experimental evidence for this assertion has never been obtained.

To investigate this distinction, we have used a double-notched four-point bend test, which consists of a rectangular bar containing two nominally identical rounded notches (root radius ~200 μm) subjected to four-point bending. The basis of the test is that, with a rounded notch in the presence of some degree of inelasticity or yielding, although the maximum local strains are located at the root of the notch[2], the relaxation of stresses in the inelastic ('yielded') zone surrounding the notch results in the maximum local stresses being located some distance ahead of the notch, towards the elastic–inelastic interface[10] (Fig. 1a). (The same is true for a sharp crack, although the point of maximum stress is much closer—with shear-driven plasticity, within two crack-opening displacements—of the crack tip). Because the two notches experience the same bending moment, when one notch breaks, the other is 'frozen' at a point immediately preceding fracture. Examination of the area in the vicinity of the unfractured notch (circled area on Fig. 1b, after fracture) thus reveals the nature of the local fracture event at the onset of failure.

It is appreciated that yielding in bone cannot be simply related to shear-driven plasticity, for example, in metals, for which the notch-field solutions in Fig. 1a were explicitly derived. Indeed, the precise nature of the inelastic constitutive behaviour of bone is not known, but clearly involves diffuse microcracking damage and plasticity in the collagen fibrils, which would be sensitive to both tensile and shear stresses (somewhat akin to pressure-dependent yielding in polymers). Despite this, most theoretical models for both deformation[11] and fracture[12] in bone use the Mises criterion, which was derived for pressure-insensitive plasticity. It is in this spirit that we use the notch-field solutions in Fig. 1a, but we recognize that the quantitative details of these fields have yet to be determined for realistic constitutive relationships in bone.

Accordingly, we examined the unbroken notches in specimens made from a cadaveric human humerus using scanning electron microscopy. The extremely small (<5 μm) size of the precursor cracks that were imaged in all orientations (Fig. 1c) leaves little doubt that crack

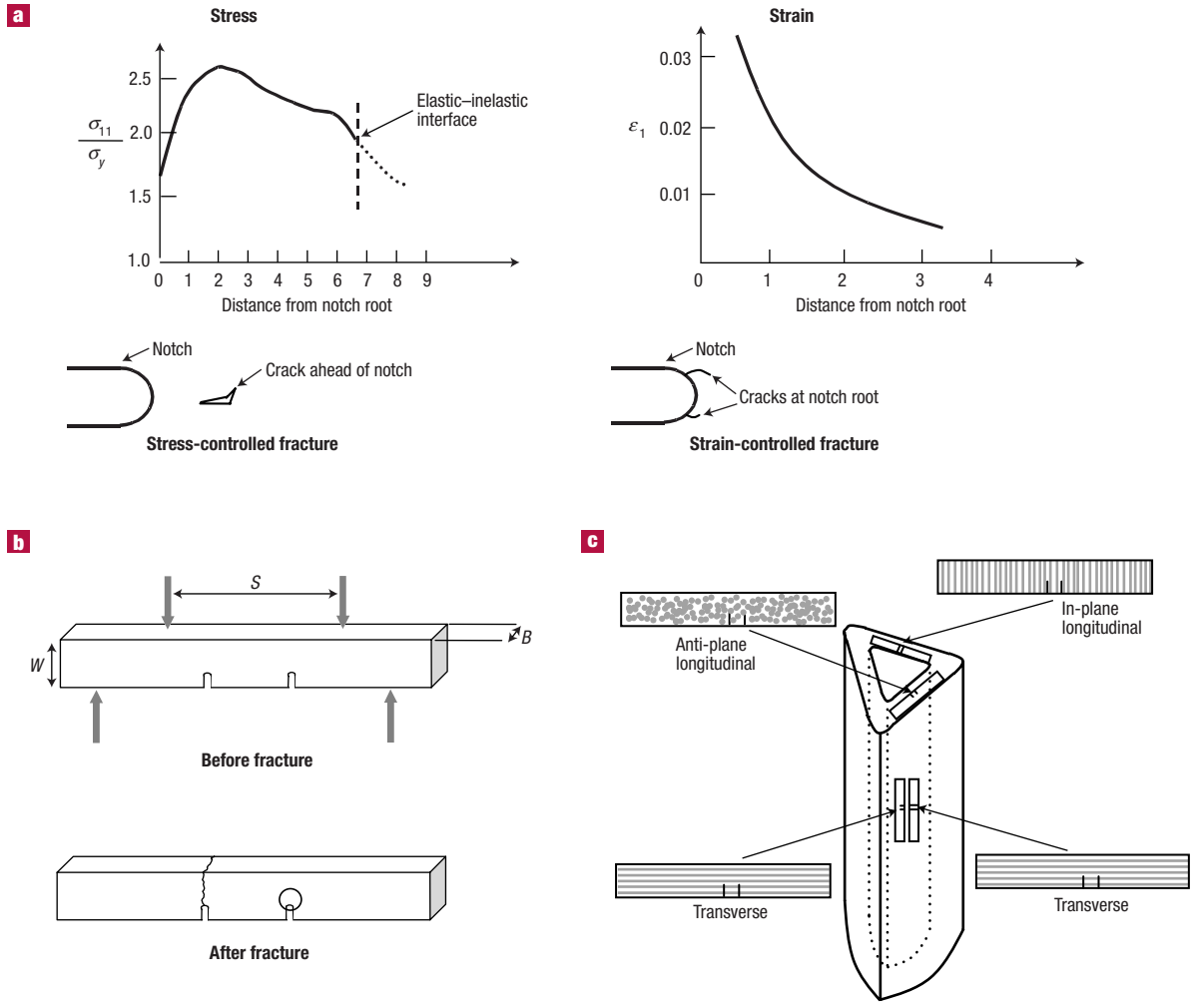

Figure 1 The difference between failure criteria, the test geometry and the orientations used. a, The stress and plastic strain distributions, based on numerical computations[10], ahead of a notch are shown, and indicate that, in the presence of any degree of inelasticity, the maximum tensile stress (σ_{11}) is ahead of the notch whereas the maximum plastic strain (ε_1) is at the notch. Consequently, a stress-controlled fracture mechanism will tend to initiate ahead of the notch, whereas the initial fracture event for strain-controlled fracture will be at the notch root. The distance from the notch root is calculated as the number of root radii. **b**, The double-notched four-point bend test used to discern whether fracture is stress- or strain-controlled. The circle indicates the area of the unfractured notch investigated for comparison (see text for discussion). Inner loading span $S \sim 10$–15 mm, sample width $W \sim 2$–3 mm, and sample thickness $B \sim 1$–3 mm. **c**, The various specimen orientations taken from the humerus (with respect to the direction of the osteons, indicated in grey) that were investigated are shown in this illustration. Short lines across the sections indicate notches along the edge, whereas lines fully crossing the sections indicate notches along the surface.

initiation is at the notch and not ahead of it (Fig. 2). Moreover, using previously developed techniques[10] assuming a plasticity-based criterion, numerical analysis of the specimens at maximum load where the nominal elastic bending stress, σ_{11}, at the notch was in the 40–100 MPa range (ratio of nominal stress to yield stress of $\sigma_{11}/\sigma_y \sim 0.53$–$1.33$), suggests that the tensile stresses should peak well ahead of the notch (at ~100–360 μm ahead of the notch tip, that is, at a distance of 0.5–1.2 times the notch-root radius). Because absolutely no evidence of any precursor cracking was found in this region, and all initial cracks were detected exactly at the notch root, our observations are consistent with fracture in bone being associated with a strain-based criterion.

Insights into the mechanisms of fracture in bone and how it derives its toughness were also obtained from these experiments. Various toughening mechanisms have been proposed for bone. At large length-scales, the generation of 'microdamage' from microcracking (small cracks of up to hundreds of micrometres in size) has been suggested as a source of toughening in bone, specifically through crack-tip shielding[13–15]. In addition, the cement lines (at the secondary osteon boundaries) and the interlamellar boundaries are believed to provide weak interfaces to deflect the crack path and accordingly increase the toughness[16]. More recently, a role for collagen fibrils has been postulated[17–19], with fibre bridging proposed as a possible toughening mechanism[20]. Indeed, toughening at the fibrillar level would explain the apparent correlation of toughness with collagen denaturation, which appears to weaken bone, and crosslinks, which appear to increase its toughness[21], although it is probable that many of these mechanisms operate in concert.

Scanning electron micrographs of the fracture paths in human bone, specifically indicating how the crack interacts with the microstructure, are shown in Fig. 3. Figure 3a shows a roughly 1-mm-long crack propagating out of the notch in the 'anti-plane longitudinal' orientation, that is, the plane of the crack and the crack front are nominally parallel to the long axis of the osteons. It is apparent that at this scale of observation, the most recognizable features of the microstructure, the Haversian canals (dark region within each osteon) with their concentric lamellar rings, do not have a major influence on

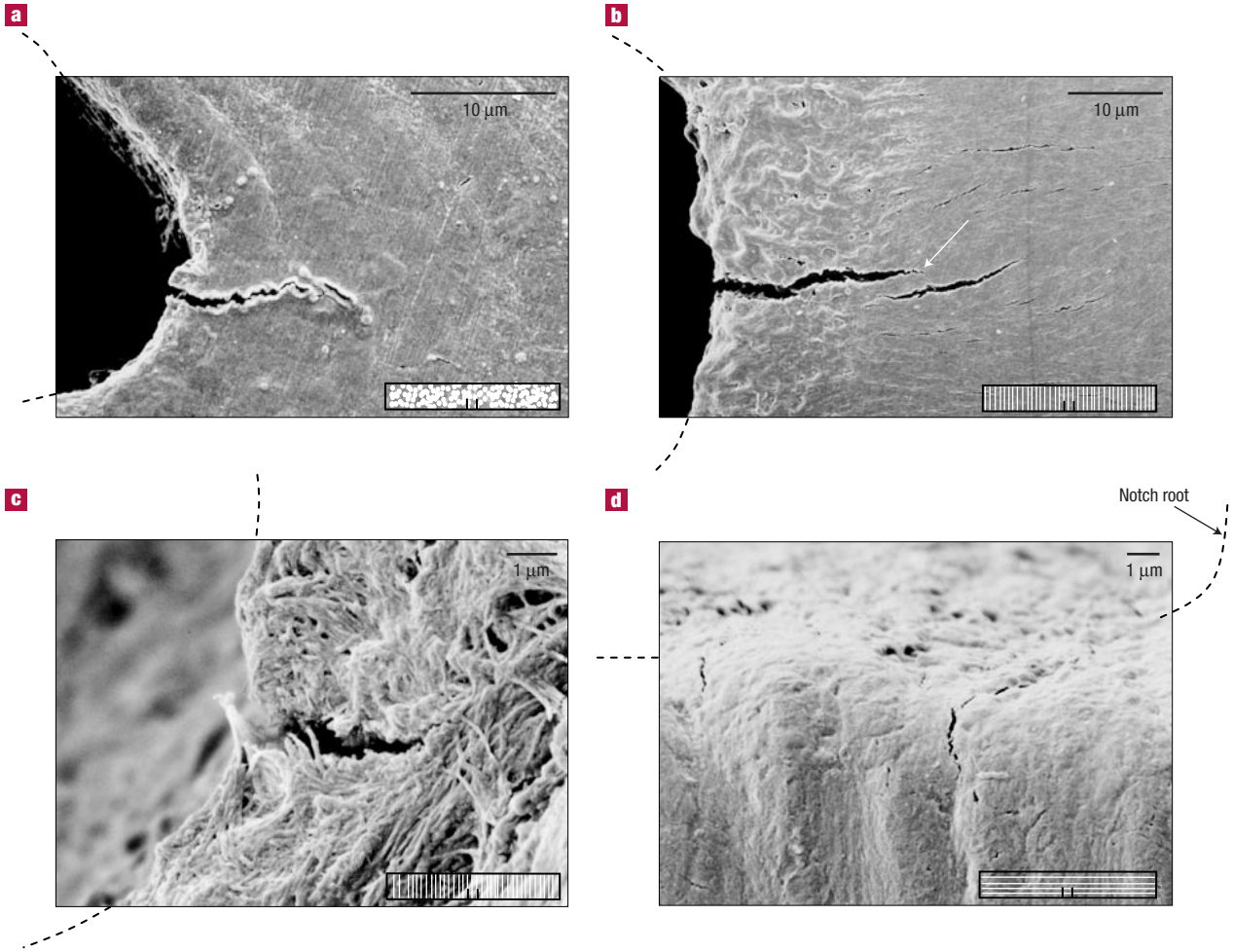

Figure 2 Scanning electron micrographs of the area near the unbroken notch for various orientations. a, A crack emanating directly from the notch root in the 'anti-plane longitudinal' orientation. **b**, Associated evidence of uncracked ligament bridging (indicated by white arrow) and of extensive microcracking for the 'in-plane longitudinal' orientation. **c**, The extremely small (<5 μm) size of the precursor cracks like the one shown here leaves little doubt that crack initiation is at the notch and not ahead of it, consistent with the notion of locally strain-controlled fracture. **d**, The strong influence of the underlying microstructure can lead to cracks emanating well behind the notch root, as illustrated here for the 'transverse' orientation. Also, multiple crack initiation can be seen. The dashed lines indicate the notch surface. The insets show the specimen orientation with respect to the direction of the osteons.

the path taken by the growing crack. Investigation of the near-tip region of this crack, however, shown by the white circle, revealed evidence of so-called uncracked-ligament bridging, as indicated by the white arrows in Fig. 3b. This is an extrinsic toughening mechanism involving two-dimensional uncracked regions along the crack path that can bridge the crack on opening; it is commonly seen in metal–matrix composites[22] and intermetallics such as γ-based TiAl[23]. Such uncracked-ligament bridging, however, is more prominent in the in-plane longitudinal orientation, as shown by the white arrow in Fig. 2b, where evidence of microcracking is also apparent near the crack. This can also lead to extrinsic toughening through its effect in creating dilation and reducing the modulus in the region surrounding the crack. For the anti-plane longitudinal orientation, a third mechanism of toughening in bone can be seen in Fig. 3c in the form of crack-bridging by the collagen fibrils.

However, for the transverse specimen orientations, where the osteons run along the specimen length (Fig. 1c), we observed a much stronger influence of the underlying microstructure on the crack path. Crack initiation and initial crack growth out of the notch was not in the direction normal to the maximum tensile stress, but rather in the direction of the osteons (Fig. 2d), consistent with the suggestion[16] that the osteonal cement lines, which are the interface between the osteonal system and the surrounding matrix, can provide a weak path for the propagation of the crack (as shown in Fig. 3d by the deflected cracks emanating from the notch root). The resulting large out-of-plane crack deflections can lead to substantial toughening (as estimated below) and must be considered as a leading factor associated with the marked anisotropy in the fracture properties of cortical bone.

Such notions on the mechanisms of toughening in bone and how they vary with orientation are consistent with our fracture-toughness measurements. Using fatigue-precracked bend samples, we measured fracture-toughness values of K_c = 5.33 (± 0.41) MPa $m^{1/2}$ for the transverse orientation, as compared to 2.21 (± 0.18) MPa $m^{1/2}$ for anti-plane longitudinal orientation and 3.53 (± 0.13) MPa $m^{1/2}$ for the in-plane longitudinal orientation. This is consistent with previous results that give the toughness of bone to be between 2 – 8 MPa $m^{1/2}$ (refs 24–26) and to be higher in the transverse direction[24,25,27].

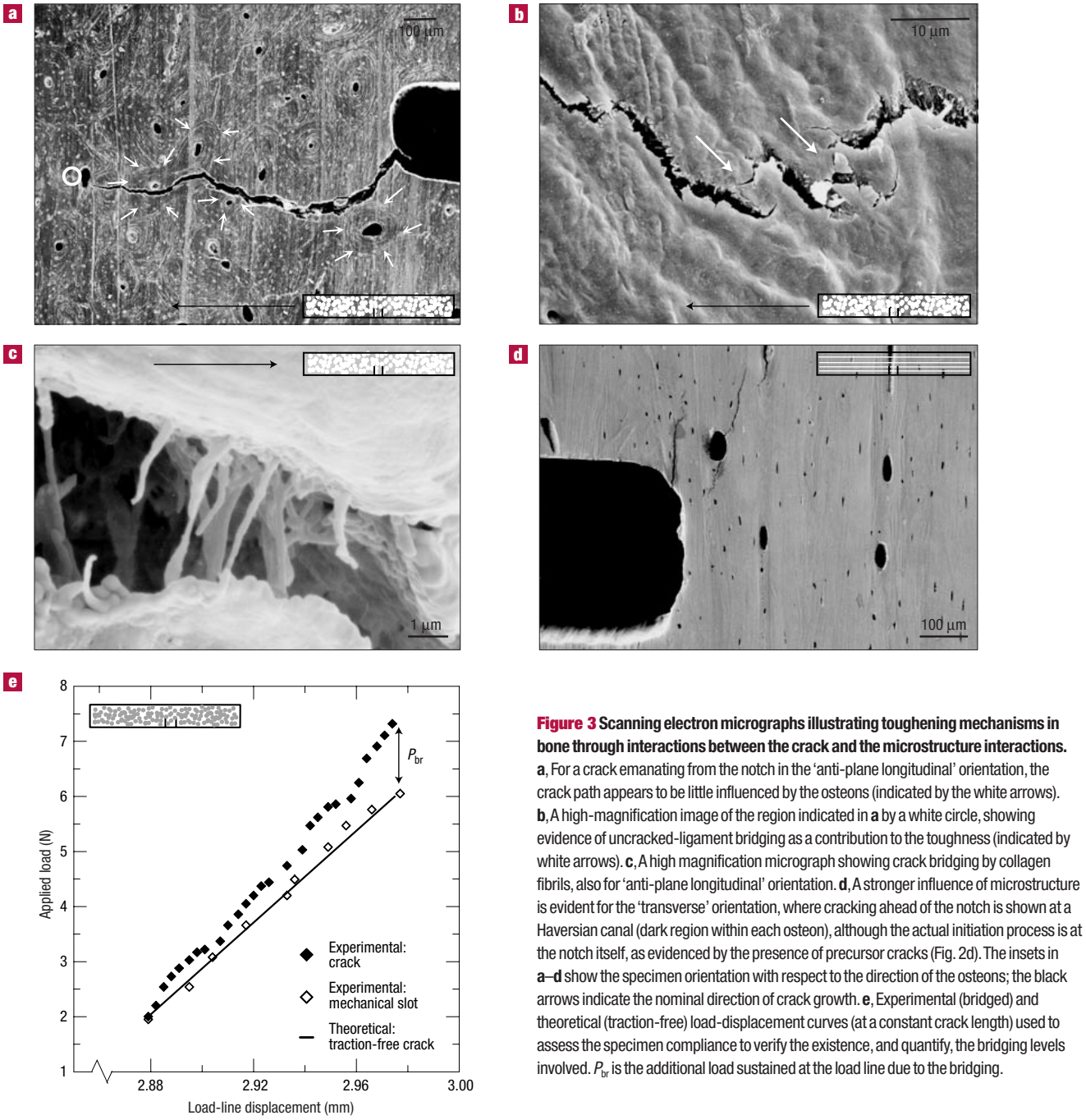

Figure 3 Scanning electron micrographs illustrating toughening mechanisms in bone through interactions between the crack and the microstructure interactions. **a**, For a crack emanating from the notch in the 'anti-plane longitudinal' orientation, the crack path appears to be little influenced by the osteons (indicated by the white arrows). **b**, A high-magnification image of the region indicated in **a** by a white circle, showing evidence of uncracked-ligament bridging as a contribution to the toughness (indicated by white arrows). **c**, A high magnification micrograph showing crack bridging by collagen fibrils, also for 'anti-plane longitudinal' orientation. **d**, A stronger influence of microstructure is evident for the 'transverse' orientation, where cracking ahead of the notch is shown at a Haversian canal (dark region within each osteon), although the actual initiation process is at the notch itself, as evidenced by the presence of precursor cracks (Fig. 2d). The insets in **a**–**d** show the specimen orientation with respect to the direction of the osteons; the black arrows indicate the nominal direction of crack growth. **e**, Experimental (bridged) and theoretical (traction-free) load-displacement curves (at a constant crack length) used to assess the specimen compliance to verify the existence, and quantify, the bridging levels involved. P_{br} is the additional load sustained at the load line due to the bridging.

These observations and measurements can be verified by experiment and theory. The highest toughness is in the transverse orientation, where the crack path deflects at 90 degrees to the plane of maximum tensile stress, that is along a path parallel to the notch root (Fig. 3d). Linear-elastic calculations using crack-deflection mechanics[28,29] suggest that for such an in-plane deviation of the crack path, the stress intensity experienced at the crack tip would be reduced by some 50% compared to that for an undeflected crack, consistent with the toughness being approximately twice as high in this orientation. A smaller toughening effect is seen in the in-plane longitudinal orientation where crack bridging by uncracked ligaments (and collagen fibrils) is apparent (Fig. 3b). To verify whether such bridging is effective, we compared measurements of the elastic compliance (inverse stiffness) of the cracked bone to those made where we had subsequently machined out the wake of the crack; we also verified the latter measurements by showing that they were identical to the theoretical compliance for a traction-free crack of the same size[30]. Results for the anti-plane longitudinal orientation are shown in Fig. 3e, and clearly indicate that the crack in the bone has a lower compliance than a traction-free crack of identical length. Such results provide strong evidence that cracks in human bone are indeed bridged.

We can quantify the effect of this on the toughening in bone from the difference between the two curves at maximum load, which gives the additional load sustained at the load-line, P_{br} (of value ~1.5 N), due to the presence of the bridges. This equates to a bridging stress intensity, K_{br}, and hence a contribution to the toughness, of ~0.5 MPa $m^{1/2}$, that is, a quarter of K_c for this orientation. In comparison, theoretical estimates

of ligament bridging, based on a limiting crack-opening approach[22], yield values of $K_{br} \sim 0.3$ MPa $m^{1/2}$. Such experimental measurements, coupled with the theoretical estimates, strongly suggest that uncracked-ligament bridging provides a finite contribution to the toughening of bone.

Thus in summary, we have shown by novel experimentation that the local criterion for fracture in human cortical bone is consistent with a strain-based criterion. We believe that this is the first direct experimental evidence for the validity of the assumption of a strain-based criterion, which has been widely used in theoretical models of the mechanical behaviour of bone[3]. In addition, we have shown that the marked anisotropy in the toughness properties of bone can be rationalized in terms of several extrinsic toughening mechanisms induced by specific features in the microstructure. Indeed, through compliance analysis we provide the first quantitative measurements of the contribution to bone toughening from crack bridging. These results are of special interest in that they form the basis of physically based micromechanistic understanding of the fracture and failure of human cortical bone.

METHODS

DOUBLE-NOTCH EXPERIMENTS

A fresh-frozen human cadaveric humerus from a 34-year-old female was used; the cause of death was unrelated to the condition of the extracted bone. Tests were conducted using a symmetric four-point bending geometry (inner loading span $S \sim 10$–15 mm, sample width $W \sim 2$–3 mm) with a double rounded-notched configuration (Fig. 1b). Rounded notches (root radius 200–300 μm, and depth 0.3–0.4 W) were introduced with a slow speed saw; care was taken to maintain the specimens in a hydrated state throughout the specimen preparation and testing process. The depths of both notches in each specimen were kept as identical as possible in order to ensure similar stress–strain fields at the notch tips. A total of eighteen such tests were conducted (at least three for each of the orientations used—see Fig. 1c). All testing was conducted at ambient temperature on an ELF3200 series voice coil-based mechanical testing machine (EnduraTEC, Minnetonka, Minnesota, USA). The bend bars were loaded to failure under displacement control at a constant cross-head movement rate of 0.01 mm sec^{-1}. The area around the unfractured notch (Fig. 1b, after fracture) was examined using a high-power optical microscope and (after coating with a gold–palladium alloy) with a scanning electron microscope operating in the back-scattered electron mode.

FRACTURE-TOUGHNESS MEASUREMENTS

Fracture-toughness testing was performed in general accordance with the ASTM Standard[31]. Tests were conducted using the notched three-point bending geometry with a span between the lower two loading points equal to 5–5.5 times the width of the beam. Longitudinal and transverse orientations were investigated. The notch was 'sharpened' by precracking using cyclic fatigue loading; this was achieved at a load ratio (ratio of minimum to maximum loads) of 0.1 and loading frequency of 2 Hz, with a final maximum stress intensity of $K_{max} \sim 1$–2 MPa $m^{1/2}$. The final precrack length (notch plus precrack) was generally ~0.4–0.6 W, with a presumed atomically sharp crack tip. Samples were then loaded to failure under displacement control with an ELF testing machine at ambient temperature at a cross-head displacement rate of 0.01 mm sec^{-1}. A record of the applied loads and the corresponding displacements was simultaneously monitored during the test and analysed to determine the fracture toughness. At least three separate specimens were tested for each orientation. Linear-elastic stress intensities, K, were computed from handbook solutions for three-point bending[31].

CRACK-BRIDGING EXPERIMENTS

To confirm the presence of crack bridging in bone, four experiments were performed where a crack was grown from a rounded notch in a three-point bend specimen to a certain length between 1 and 1.5 mm. The measured compliance of this crack was then determined by monitoring the load-line displacement as a function of applied bending load. This was then compared to the theoretical compliance for a traction-free crack of identical length in this geometry[32]. To check the veracity of the theoretical estimate for the case of bone, we machined out the wake of the crack using a slow-speed diamond saw to obtain a nominally traction-free crack of the same length, and measured its compliance (see Fig. 3e). The width of this saw cut (~300 μm) has no effect on the measured compliance.

Received 18 November 2002; accepted 13 January 2003; published 9 February 2003.

References

1. Ritchie, R. O., Knott, J. F. & Rice, J. R. On the relationship between critical tensile stress and fracture toughness in mild steel. *J. Mech. Phys. Solids* **21,** 395–410 (1973).
2. Ritchie, R. O., Server, W. L. & Wullaert, R. A. Critical fracture stress and fracture strain models for the prediction of lower and upper shelf toughness in nuclear pressure vessel steels. *Metall. Trans. A* **10,** 1557–1570 (1979).
3. Yeh, O. C. & Keaveny, T. M. Relative roles of microdamage and microfracture in the mechanical behaviour of trabecular bone. *J. Orthopaed. Res.* **19,** 1001–1007 (2001).
4. Keyak, J. H. & Rossi, S. A. Prediction of femoral fracture load using finite element models: an examination of stress- and strain-based failure theories. *J. Biomech.* **33,** 209–214 (2000).
5. Lewandowski J. J. & Thompson A. W. in *Advances in Fracture Research (Fracture 84): Proc. 6th Int. Conf. on Fracture* (ed. Valluri, S. R.) 1515–1522 (Pergamon, New York, USA, 1984).
6. http://ttb.eng.wayne.edu/~grimm/ME518/L3F3.html, from Park, J. B. & Lakes, R. S. *Biomaterials: An Introduction* (Plenum, New York, USA, 1992).
7. Rho, J. Y., Kuhn-Spearing, L. & Zioupos, P. Mechanical properties and the hierarchical structure of bone. *Med. Eng. Phys.* **20,** 92–102 (1998).
8. Weiner, S. & Wagner, H. D. The material bone: Structure-mechanical function relations. *Annu. Rev. Mater. Sci.* **28,** 271–298 (1998).
9. Currey, J. D. 'Osteons' in biomechanical literature. *J. Biomech.* **15,** 717 (1982).
10. Griffiths, J. R. & Owen, D. R. J. An elastic-plastic stress analysis for a notched bar in plane strain bending. *J. Mech. Phys. Solids* **19,** 419–431 (1971).
11. Zioupos, P., Currey, J. D., Mirza, M. S. & Barton, D. C. Experimentally determined microcracking around a circular hole in a flat plate of bone: comparison with predicted stresses. *Phil. Trans. R. Soc. Lond. B.* **347,** 383–396 (1995).
12. Lotz, J. C., Cheal, E. J. & Hayes, W. C. Fracture prediction for the proximal femur using finite element models: Part I - Linear analysis. *J. Biomech. Eng.* **113,** 353–360 (1991).
13. Vashishth, D. *et al.* In vivo diffuse damage in human vertebral trabecular bone. *Bone* **26,** 147–152 (2000).
14. Parsamian G. P. & Norman, T. L. Diffuse damage accumulation in the fracture process zone of human cortical bone specimens and its influence on fracture toughness, *J. Mater. Sci.: Mater. Med.* **12,** 779–783 (2001).
15. Vashishth, D., Tanner, K. E. & Bonfield, W. Contribution, development and morphology of microcracking in cortical bone during crack propagation *J. Biomech.* **33,** 1169–1174 (2000).
16. Yeni, Y. N. & Norman, T. L. Calculation of porosity and osteonal cement line effects on the effective fracture toughness of cortical bone in longitudinal crack growth. *J. Biomed. Mater. Res.* **51,** 504–509 (2000).
17. Wang, X., Bank, R. A., Tekoppele, J. M. & Agrawal, C. M. The role of collagen in determining bone mechanical properties. *J. Orthopaed. Res.* **19,** 1021–1026 (2001).
18. Wang, X., Shen, X., Li, X. & Agrawal, C. M. Age-related changes in the collagen network and the toughness of bone. *Bone* **31,** 1–7 (2002).
19. Thompson, J. B. *et al.* Bone indentation recovery time correlates with bond reforming time. *Nature* **414,** 773–776 (2001).
20. Yeni, Y. N. & Fyhrie, D. P. in *Proc. Bioeng. Conf. BED* Vol. 50 293–294 (ASME, New York, USA, 2001).
21. Burr, D. B. The contribution of the organic matrix to bone's material properties. *Bone* **31,** 8–11 (2002).
22. Shang, J. H. & Ritchie, R. O. Crack bridging by uncracked ligaments during fatigue-crack growth in SiC-reinforced aluminum-alloy composites. *Metall. Trans. A* **20,** 897–908 (1989).
23. Campbell, J. P., Venkateswara Rao, K. T. & Ritchie, R. O. The effect of microstructure on fracture toughness and fatigue crack growth behaviour in γ-titanium aluminide based intermetallics. *Metall. Mater. Trans. A* **30,** 563–577 (1999).
24. Phelps, J. B., Hubbard, G. B., Wang, X. & Agrawal, C. M. Microstructural heterogeneity and the fracture toughness of bone. *J. Biomed. Mater. Res.* **51,** 735–741 (2000).
25. Lucksanambool, P., Higgs, W. A. J., Higgs, R. J. E. D. & Swain, M. W. Fracture toughness of bovine bone: influence of orientation and storage media. *Biomater.* **22,** 3127–3132 (2001).
26. Zioupos, P. & Currey, J. D. Changes in the stiffness, strength, and toughness of human cortical bone with age. *Bone* **22,** 57–66 (1998).
27. Behiri, J. C. & Bonfield, W. Orientation dependence on fracture mechanics of bone. *J. Biomech.* **22,** 863–872 (1989).
28. Bilby, B. A., Cardew, G. E. & Howard, I. C. in *Fracture 1977* (ed. Taplin, D. H. R.) Vol. 3 197–200 (Pergamon, Oxford, UK, 1978).
29. Cotterell, B. & Rice, J. R. Slightly curved or kinked cracks. *Int. J. Fract.* **16,** 155–169 (1980).
30. Ritchie, R. O., Yu, W. & Bucci, R. J. Fatigue crack propagation in ARALL laminates: measurement of the effect of crack-tip shielding from crack bridging. *Eng. Fract. Mech.* **32,** 361–377 (1989).
31. ASTM E 399–90 (Reapproved 1997). *Annual Book of ASTM Standards, Vol. 03.01: Metals- Mechanical Testing; Elevated and Low-temperature Tests; Metallography* (ASTM, West Conshohocken, Pennsylvania, USA, 2001).
32. Haggag, F. M. & Underwood, J. H. Compliance of a three-point bend specimen at load line. *Int. J. Fract.* **26,** 63–65 (1984).

Acknowledgements

This work was supported by the National Institutes of Health under Grant No. P01DE09859 (for R.K.N.) and by the Office of Science, Office of Basic Energy Science of the Department of Energy under Contract No. DE-Ac03-76SF00098 (for R.O.R.). The authors wish to thank Christian M. Puttlitz (University of California, San Francisco) for supplying the human bone used in this study, Jamie J. Kruzic for assistance with the compliance measurements, and John W. Hutchinson for helpful discussion.
Correspondence and requests for materials should be addressed to R.O.R.

Competing financial interests

The authors declare that they have no competing financial interests.